

# Polarization fatigue in $\text{Pb}(\text{Zn}_{1/3}\text{Nb}_{2/3})\text{O}_3\text{-PbTiO}_3$ ferroelectric single crystals

Metin Ozgul, Koichi Takemura,<sup>a)</sup> Susan Trolier-McKinstry, and Clive A. Randall<sup>b)</sup>

Center for Dielectric Studies, Materials Research Laboratory, The Pennsylvania State University, University Park, Pennsylvania 16802-4800

(Received 9 June 2000; accepted for publication 2 November 2000)

$\text{Pb}(\text{Zn}_{1/3}\text{Nb}_{2/3})\text{O}_3\text{-PbTiO}_3$  (PZN-PT) single crystal ferroelectrics have been studied to determine the relative rates of polarization fatigue. It was recently found that ferroelectrics with the rhombohedral phase in the PZN-PT solid solution have essentially no polarization fatigue in the  $[001]_C$  directions (all of the orientations in this article will be given in terms of the prototype cubic ( $m3m$ ) axes, denoted by the subscript  $C$ ). In this study, we expand upon this observation to correlate fatigue rates more completely with respect to composition, orientation, temperature, and electric field strength. It is inferred that an engineered domain state in relaxor based ferroelectric crystals with the spontaneous polarization inclined to the normal of the electrode is associated with negligible or no fatigue at room temperature. However, if thermal history, temperature, or field strength induces a phase transition that produces a polarization parallel to the normal of electrode, these orientations fatigue. The relative fatigue rates are also studied as a function of temperature. In directions, such as  $[111]_C$  in the ferroelectric rhombohedral phase, the polarization fatigues at room temperature, but as temperature is increased the fatigue rate systematically decreases. This is explained in terms of a thermally activated process that limits the net fatigue rate of ferroelectrics. In summary, this article gives information on the polarization states and orientation that control fatigue in ferroelectric crystals with a relaxor end member. © 2001 American Institute of Physics. [DOI: 10.1063/1.1335819]

## I. INTRODUCTION

Ferroelectric fatigue is the systematic reduction of switchable polarization in a ferroelectric material undergoing bipolar drive. Figure 1 shows a schematic of the polarization decay in a ferroelectric material as a function of the number of cycles and also the corresponding evolution of the hysteresis loops. This phenomenon has received a great deal of investigation over the past ten years to aid the development of thin film ferroelectric random access memories. Fatigue is generally agreed to be the result of charge injection and the accumulation of space charge that pins domain walls or retards the nucleation of reversed domains to permit switching.<sup>1-11</sup>

There have been a number of strategies used to improve fatigue resistance in ferroelectrics; these include:

- (i) Doping the ferroelectric with donor dopants, e.g.,  $\text{La}^{12,13}$  or  $\text{Nb}^{14}$  in  $\text{Pb}(\text{Zr,Ti})\text{O}_3$  (PZT).
- (ii) Oxide electrodes,  $\text{RuO}_2$ ,<sup>15-17</sup>  $\text{IrO}_2$ ,<sup>18,19</sup>  $\text{SrRuO}_3$ ,<sup>20</sup> and  $(\text{La,Sr})\text{CoO}_3$ ,<sup>21-23</sup> for PZT thin film ferroelectrics.
- (iii) Nonfatiguing ferroelectrics with Pt electrodes, e.g.,  $\text{SrBi}_2\text{Ta}_2\text{O}_9$  or  $\text{SrBi}_2\text{Nb}_2\text{O}_9$ .<sup>24-26</sup>

Our recent studies have explored a fourth possible method to resist fatigue, namely, the use of domain engineering and crystal anisotropy.<sup>27-29</sup> In this case, the spontaneous polarization vectors are inclined relative to the normal of the electrode plane. The objective of this article is to build upon

the domain engineering and crystal orientation studies, which were previously confined to room temperature fatigue rates, and field levels that did not induce ferroelectric-ferroelectric phase switching. Here we are concerned with the influence of temperature and phase transitions on fatigue rates in crystals measured in different directions and with compositions.

## II. EXPERIMENTAL PROCEDURE

The ferroelectric system selected for this study is the  $\text{Pb}(\text{Zn}_{1/3}\text{Nb}_{2/3})\text{O}_3\text{-PbTiO}_3$  (PZN-PT) solid solution. This is a perovskite material with lead occupying the twelfold coordinated site, and Zn-Nb and Ti occupying the octahedral site with intermediate scale cation ordering, depending on Ti content.<sup>30</sup> PZN-PT single crystals are of interest owing to their extraordinary piezoelectric properties (piezoelectric coefficients  $d_{33} \approx 2500$  pC/N and electromechanical coupling coefficients  $K_p^2 \geq 90\%$  in the  $[001]_C$  direction in the rhombohedral ferroelectric phase).<sup>31</sup>

Crystals of  $(1-x)\text{PZN}-x\text{PT}$  ( $x=0.00, 0.045, 0.080, 0.10, \text{ and } 0.12$ ) were grown using the high temperature flux technique.<sup>32</sup> As shown in Fig. 2, PZN and PZN-4.5PT crystals are rhombohedral (pseudocubic) at room temperature. As the PT increased beyond 8%, the composition of crystals approaches to the morphotropic phase boundary (MPB) separating rhombohedral and tetragonal ferroelectric phases. PZN-8PT crystals are in the rhombohedral phase field but PZN-10PT crystals are close to the phase boundary at room temperature and therefore small chemical inhomogeneities in the crystal will lead to mixed phases. PZN-12PT crystals are in a tetragonal ferroelectric phase field at room temperature.

<sup>a)</sup>Present address: ULSI Device Development Division, NEC Electron Devices, NEC Corporation, 1120 Shimokuzawa, Sagami-hara 229-1198, Japan.

<sup>b)</sup>Electronic mail: CAR4@PSU.EDU

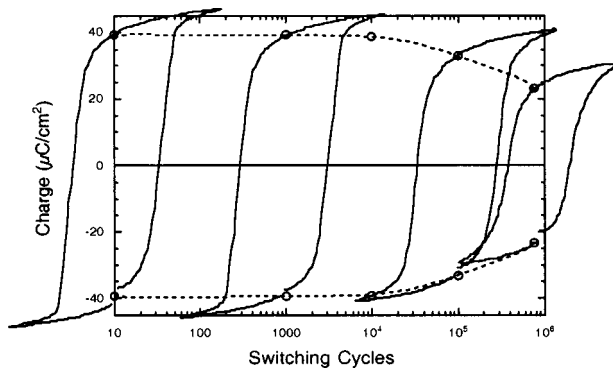


FIG. 1. A schematic illustration of polarization decay as a function of the number of the switching cycles.

The crystal samples were oriented along the  $[111]_C$ ,  $[110]_C$ , and  $[001]_C$  axes within  $\pm 2^\circ$  by using a Laue Camera (Multiware Laboratories Ltd., real-time Laue machine).

For electrical characterization, plate-shape samples were cut off from the oriented samples and prepared by polishing with silicon carbide and alumina polishing powders (down to  $\sim 1 \mu\text{m}$ ) to achieve flat and parallel surfaces onto which silver paste electrodes were applied. Silver paste electrodes were preferred due to the fact that they can be removed easily by washing with acetone without changing the nature of the crystal/electrode interface after the experiments although similar results are obtained with Pt electrodes.<sup>27,29</sup> The thickness of samples used in this study ranged from  $200 \mu\text{m}$  to  $1 \text{mm}$ .

High field measurements including polarization and strain hysteresis utilized a modified Sawyer–Tower circuit and linear variable differential transducer driven by a lock-in amplifier (Stanford Research Systems, Model SR830). Electric fields ( $E$ ) as high as  $\sim 85 \text{ kV/cm}$  were applied in strain measurements using an amplified unipolar wave form at  $0.1 \text{ Hz}$ . In particular, the electric field was applied with a triangular bipolar wave form for the polarization switching and fatigue experiments. A high voltage dc amplifier (Trek

Model 609C-6) was used in both strain and polarization fatigue property measurements. The magnitude and the frequency of the applied ac field were generally  $20 \text{ kV/cm}$  and  $10 \text{ Hz}$ , respectively, unless otherwise stated. During measurements, the samples were submerged in Fluorinert, an insulating liquid, to prevent arcing. To study the influence of temperature on fatigue, the Fluorinert liquid was heated or cooled from the room temperature using an oven and liquid nitrogen cryostat, respectively. The experiments were performed at temperatures ranging from  $-70$  to  $150^\circ\text{C}$  depending on the crystal composition.

The remanent polarizations ( $P_r$ ) and the coercive fields ( $E_c$ ) were computed from the recorded hysteresis loops. Fatigue rate is defined as the change in remanent polarization as a function of the number of switching cycles. All the changes are given as normalized values represented as percentages of initial remanent polarization or coercive field.

### III. RESULTS AND DISCUSSION

#### A. Temperature dependence of fatigue

Figure 3 shows the virgin hysteresis loops and loops after  $10^5$  cycles at different temperatures:  $23$ ,  $65$ ,  $75$ ,  $85$ , and  $100^\circ\text{C}$ , respectively, in PZN–4.5PT crystals in  $[111]_C$  orientation. Fatigue is observed at room temperature with the first  $10^5$  cycles for a triangular ac field, amplitude  $20 \text{ kV/cm}$  and frequency  $10 \text{ Hz}$ , and for temperatures below  $85^\circ\text{C}$ . In the  $[111]_C$  rhombohedral case, the fatigue rate is reduced at higher temperatures, as shown in Fig. 4. The higher temperatures enable domain switching to overcome the pinning forces of the accumulated defects or space charge. Also at high temperatures, the probability of nucleation (or activating more preexisting nuclei) increases, thereby enabling polarization switching to occur throughout the ferroelectric crystals. Collectively, at these higher temperatures the spontaneous polarization does not fatigue at rates as fast as at lower temperatures.

Furthermore, in the case of tetragonal PZN–10PT (at  $75^\circ\text{C}$ ) crystals undergo fatigue in the  $[001]_C$  direction; again the fatigue rate is reduced as temperature is increased, for similar reasons as explained above for  $[111]_C$  directions for rhombohedral crystals at temperatures of  $75^\circ\text{C}$  and above. In the case of tetragonal PZN–PT switching studies at room temperature, the switching frequently causes microcracking, the stress fields about the microcracks can pin polarization switching and is an additional source of fatigue. In single crystal samples undergoing fatigue, it is important to separate the influence of microcracking over space charge or point defect domain pinning. This can be readily done by a heat treatment that rejuvenates the polarization switching, the thermal energy here would not repair the cracks but can redistribute point defects and space charge by diffusion. So rejuvenation of polarization infers that no microcracking is involved in the fatigue of the polarization switching.

Using rejuvenation and switching studies in a variety of compositions, temperatures and directions, it is clear that fatigue anisotropy exists in each phase. In orientations that have fast fatigue rates, this can be reduced by raising the temperature.

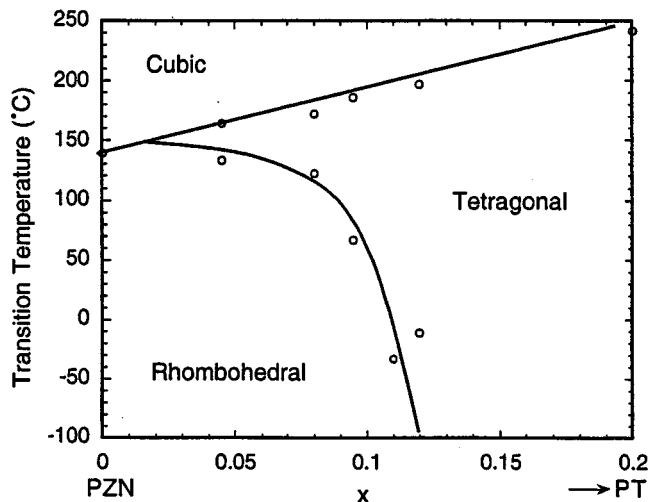


FIG. 2. Phase diagram of the  $\text{Pb}(\text{Zn}_{1/3}\text{Nb}_{2/3})\text{O}_3\text{--PbTiO}_3$  system near the MPB (from Ref. 33).

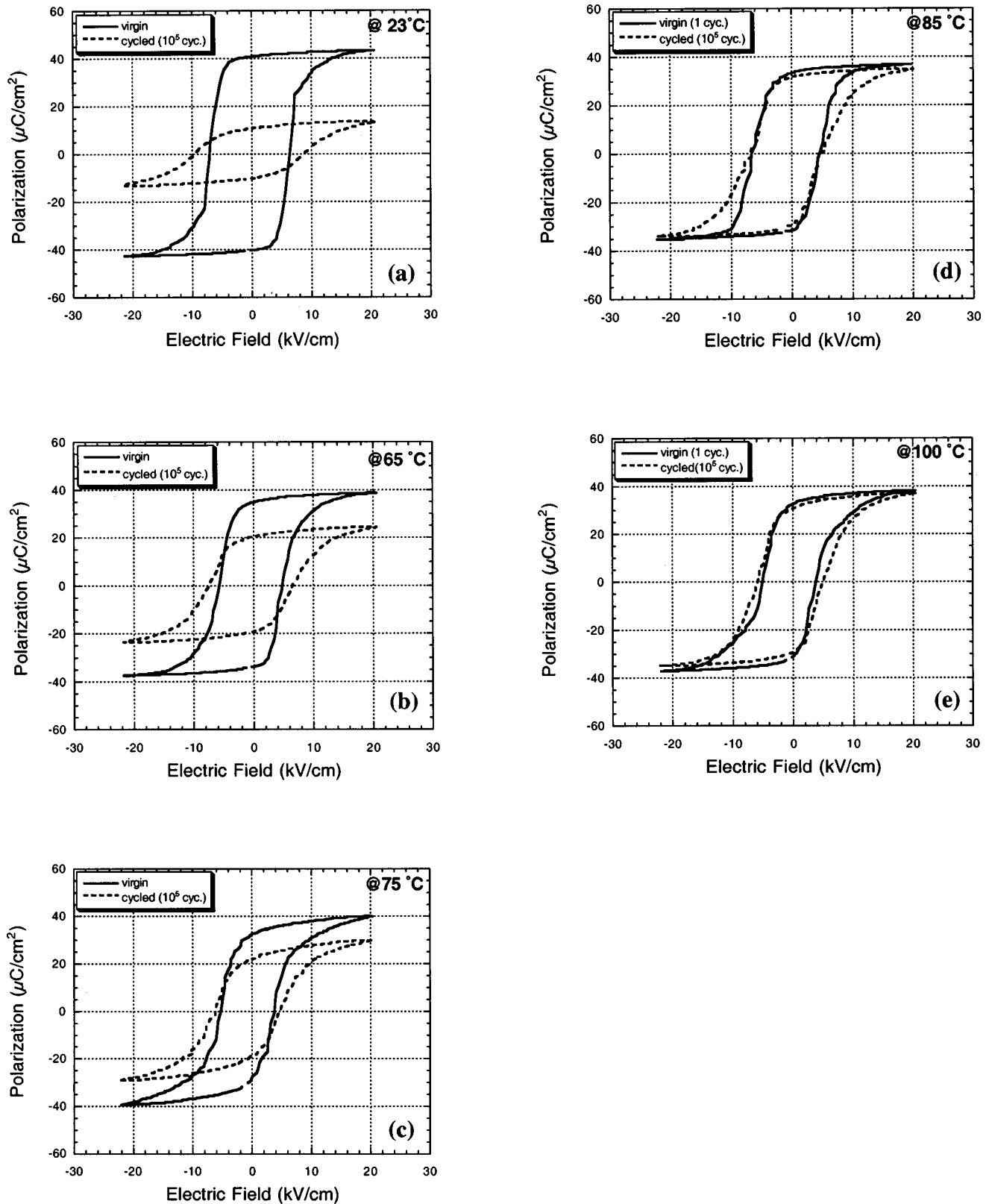


FIG. 3. The influence of switching temperature on fatigue in rhombohedral PZN-4.5PT crystal along with  $[111]_C$  orientation; (a) room temperature (23 °C), (b) 65 °C, (c) 75 °C, (d) 85 °C, and (e) 100 °C.

### B. Field induced phase transitions and their impact on fatigue rates

Figure 2 recalls the phase diagram of the PZN-PT solid solution at low temperatures and for low electric fields levels

(<1 kV/cm). In the rhombohedral phase region the  $[111]_C$  oriented crystals fatigue regardless of the applied electric field strength. In this case, the  $[111]_C$  oriented crystals have a polarization vector parallel to the electric field and switch-

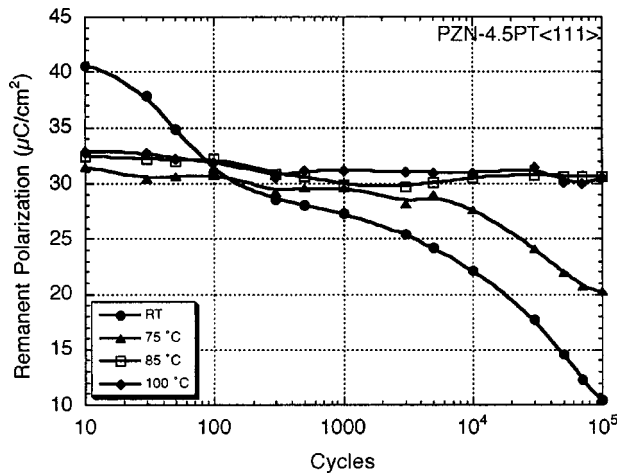


FIG. 4. A plot of fatigue rates as a function of temperature and the number of switching cycles.

ing is presumably dominated by 180° domain walls. If an electric field is applied along the [110]<sub>C</sub> and [001]<sub>C</sub> directions, the rhombohedral crystals do not show fatigue at low field strengths. In both of these cases the electric field develops an engineered domain structure with polarization vectors inclined with respect to the normal vector of the electrode plane.

However, it is known from the work of Park and co-workers<sup>34</sup> that under sufficiently high fields in specific directions, the rhombohedral ferroelectric phase can undergo field-forced phase transitions. This can change the nature of the engineered domain state; for example in the [110]<sub>C</sub> direction it is possible to induce an orthorhombic phase and in the [001]<sub>C</sub> direction a tetragonal phase can be induced at room temperatures with unipolar electric field strengths of ~15 and 30 kV/cm, respectively. High field strain versus unipolar electric field behavior is given in Fig. 5 for PZN-4.5PT crystals with [110]<sub>C</sub> orientation indicating the evi-

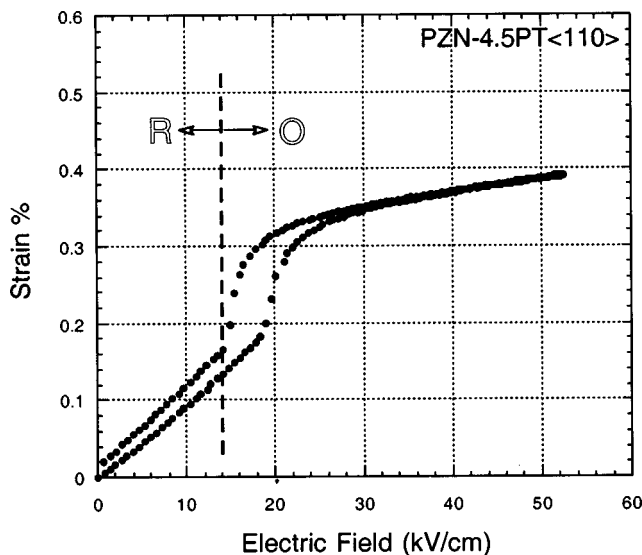


FIG. 5. High field strain vs unipolar electric field behavior for PZN-4.5PT single crystals with [110]<sub>C</sub> orientation. A high unipolar electric field induces a phase transition (rhombohedral→orthorhombic) at a critical voltage.

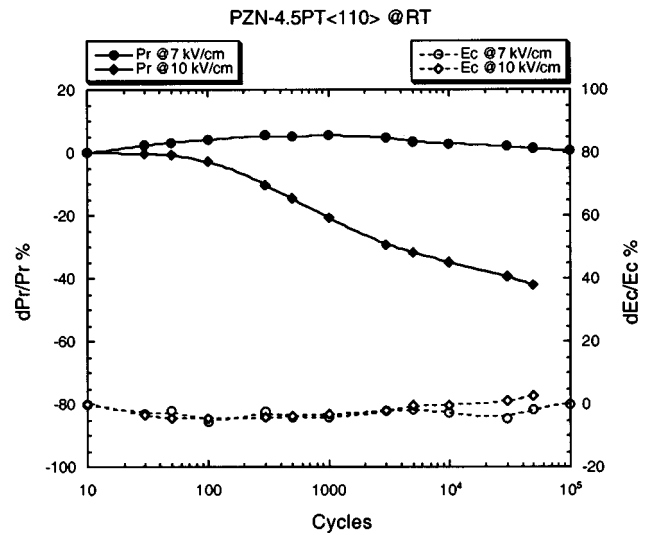
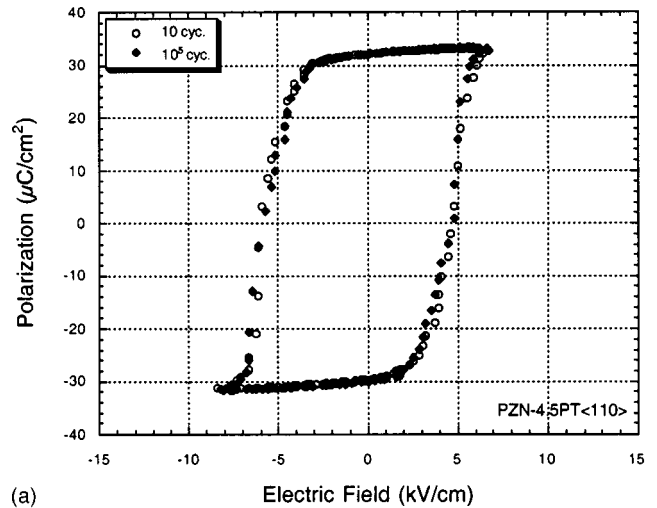
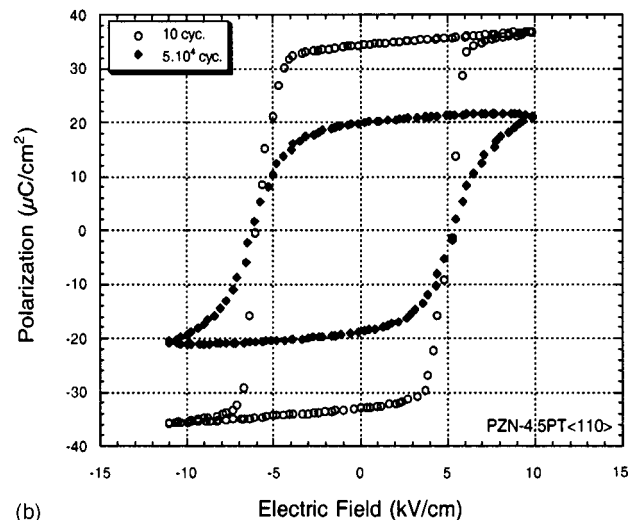


FIG. 6. Polarization fatigue behavior change in [110]<sub>C</sub> oriented PZN-4.5PT single crystals due to field induced phase switching under two different bipolar electric fields; (a) 7 kV/cm (no fatigue) and (b) 10 kV/cm (fatigue).



(a)



(b)

FIG. 7. Hysteresis loop change in PZN-4.5PT<111> single crystals after bipolar cycling below and above the critical voltage; (a) stable remanent polarization and coercive field after 10<sup>5</sup> cycles under 7 kV/cm ac field and (b) polarization fatigue after 5 × 10<sup>4</sup> cycles under 10 kV/cm ac field.

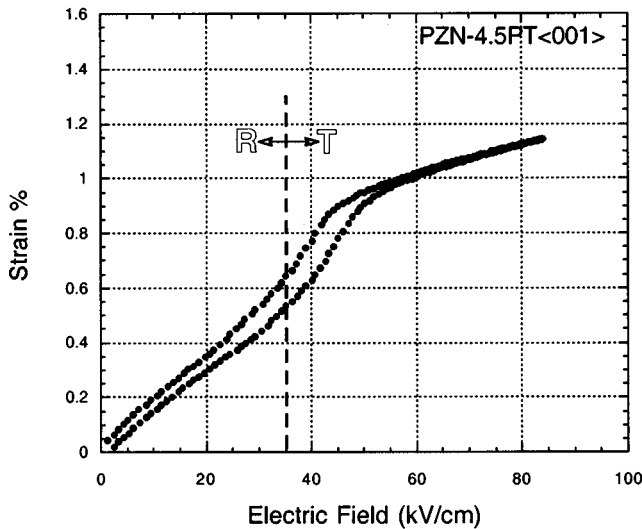


FIG. 8. High field strain vs unipolar electric field behavior for PZN-4.5PT single crystals with  $[001]_C$  orientation. A high unipolar electric field induces a phase transition (rhombohedral→tetragonal) at a critical voltage.

dence for this phase transformation. PZN-4.5PT crystals normally do not fatigue under small electric fields but show remarkable remanent polarization loss when driven at relatively higher fields as illustrated in Fig. 6. Hysteresis loops for  $[110]_C$  oriented PZN-4.5PT crystals before and after cycling under different field levels are also given in Fig. 7. Similar experiments were performed in  $[001]_C$  oriented PZN-4.5PT crystals. Even though rhombohedral PZN-4.5PT crystals do not fatigue at room temperature, very pronounced fatigue occurred under electric field levels sufficiently high to induce another phase. The unipolar strain versus field curve in Fig. 8, the remanent polarization values as a function of the number of cycles in Fig. 9, and the hysteresis behavior before and after cycling in Fig. 10 illustrate the important role of field induced phase transitions on fatigue. In the case of unipolar drive different strain-field

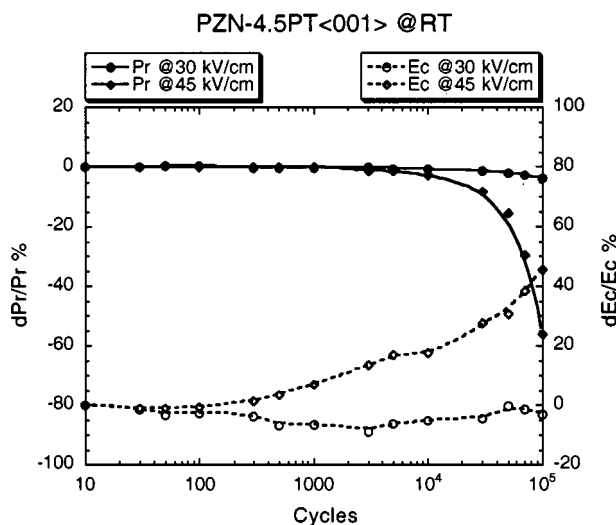


FIG. 9. Polarization fatigue behavior change in  $[001]_C$  oriented PZN-4.5PT single crystals due to field induced phase switching under two different bipolar electric fields; (a) 30 kV/cm (no fatigue) and (b) 45 kV/cm (fatigue).

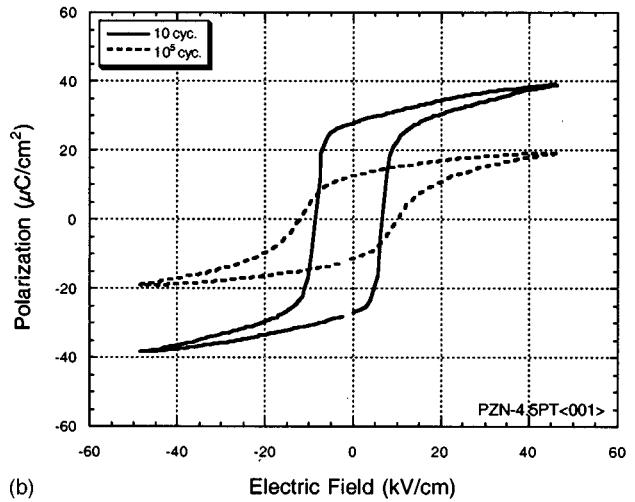
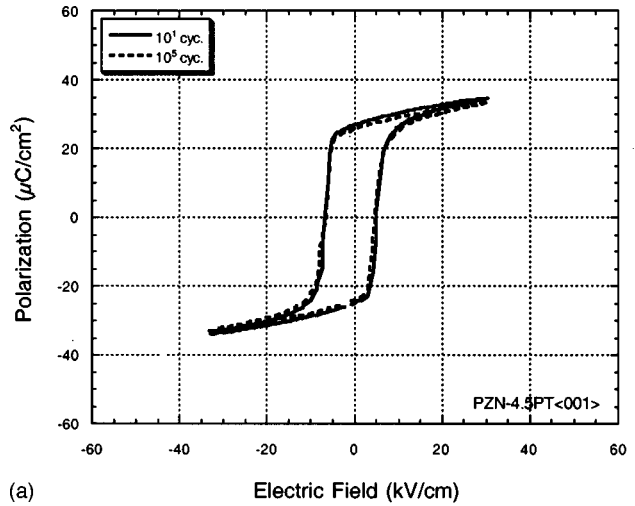


FIG. 10. Hysteresis loop change in PZN-4.5PT $(001)_C$  single crystals after bipolar cycling below and above the critical voltage; (a) stable remanent polarization and coercive field after  $10^5$  cycles under 30 kV/cm ac field and (b) polarization fatigue after  $10^5$  cycles under 45 kV/cm ac field.

slopes are noted with a hysteretic transition between the rhombohedral and field induced phase. The field levels for the transformation under unipolar conditions is higher than under ac conditions. Hysteresis losses may locally heat to enable lower temperature transitions. The transition from a ferroelectric rhombohedral to ferroelectric tetragonal (or orthorhombic) phase eventually creates a fatiguing of the crystals. The rate at which the tetragonal phase is induced from the rhombohedral phase depends on the compositions, temperature, and magnitude of the electric field. Figure 11 shows field induced fatigue in rhombohedral PZN-10PT crystal at low temperatures ( $\sim -70^\circ\text{C}$ ). The tetragonal phase is easily induced at this composition which is very close to morphotropic phase boundary. Once the remanent tetragonal phase is induced it initially causes an increase in the remanent polarization, then the fatigue process starts, and this gives a systematic reduction in the polarization as a function of cycles, above a certain number of cycles.

All of the above results suggest that, in these crystals, an engineered domain state with the polarization inclined to the

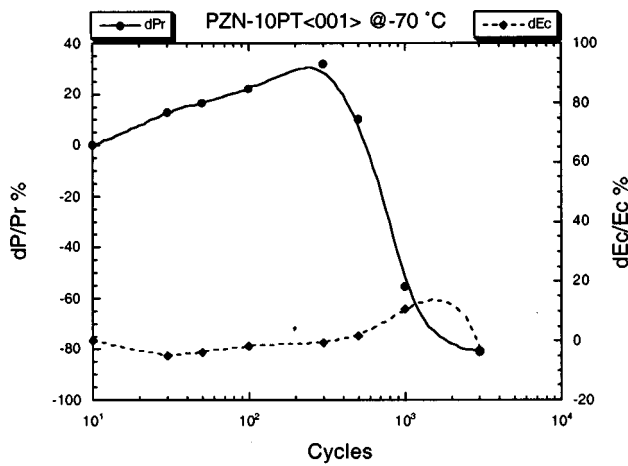


FIG. 11. Polarization fatigue behavior of PZN-10PT(001)<sub>C</sub> single crystals at ~-70 °C. The field induced tetragonal phase dominates over rhombohedral structure and produces very fast fatigue.

electrode is necessary to minimize or eliminate fatigue. This now has been confirmed at a variety of temperatures, compositions, and in both single crystal<sup>27,29</sup> and epitaxial thin film form.<sup>28</sup> The precise mechanism by which these engineered domain states limit fatigue is not understood. One possibility is that the inclined polarization states redistribute the space charge accumulation and thereby reduce the fatigue rate at a given temperature and composition. It still is under investigation, but it is also hypothesized that the engineered domain structures with the rhombohedral symmetry can have a higher percentage of charged domain walls. Charged walls could act as sinks to the injected charge in these systems. Another intriguing possibility is the multiple routes for domain switching that may exist in PZN-PT relaxor crystals, the complex dendritic domain wall structures observed under pulsed conditions indicate this great flexibility in switching paths,<sup>35</sup> and also indicate a switching process with a very high effective domain wall mobility.<sup>36</sup> This may also change the nature of the switching and thereby alter the fatigue mechanisms.

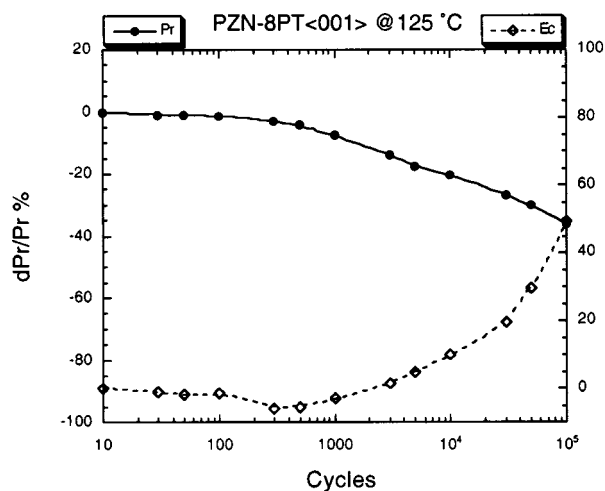


FIG. 12. Polarization fatigue behavior of PZN-8PT(001)<sub>C</sub> single crystals at 125 °C. Thermally induced tetragonal phase shows remarkable fatigue.

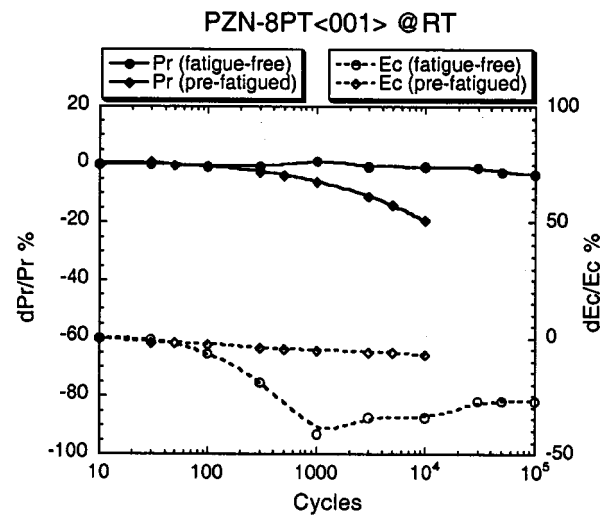


FIG. 13. Comparison of room temperature polarization fatigue behavior of PZN-8PT(001)<sub>C</sub> crystals (20 kV/cm, 10 Hz) indicating the influence of fatigue history; (a) cycled only at room temperature and (b) crystals pre-fatigued at 125 °C.

### C. Influence of fatigue history

The curved morphotropic phase boundary of the PZN-PT system permits fatigue to be studied in single crystals at different temperatures and ferroelectric phases. Crystals with composition PZN-8PT and [001]<sub>C</sub> orientation were phase induced into the tetragonal phase at 125 °C under bipolar fields with amplitude 20 kV/cm at 10 Hz. After 10<sup>5</sup> cycles, the crystal was substantially (~35%) fatigued as shown in Fig. 12. Then, these samples were cooled into the rhombohedral phase at room temperature and then driven under bipolar drive. The samples then continued to fatigue as shown in Fig. 13 in comparison with the crystal cycled only at room temperature. The fatigue at higher temperatures stabilizes local tetragonal regions, which are then cooled into

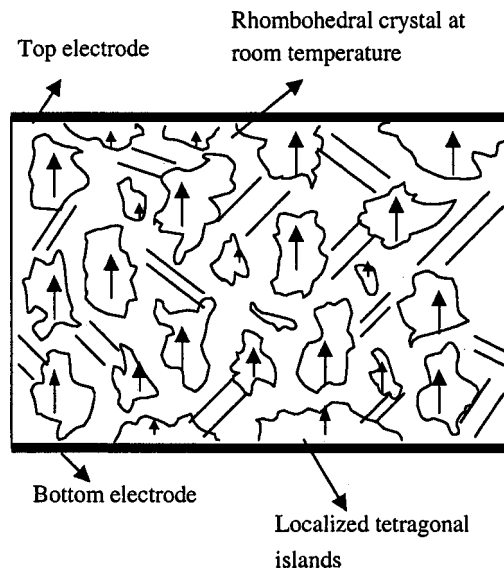


FIG. 14. A schematic illustration of room temperature mixed phase structure of PZN-8PT(001)<sub>C</sub> crystal after fatiguing at high temperature tetragonal phase region causing localized tetragonal phase stabilization.

the rhombohedral phase field, as schematically illustrated in Fig. 14. The above experiments demonstrate that there are exceptions to high temperature retardation of fatigue rates. This is the case when domain engineered crystals undergo a phase transition to produce polarization vectors parallel to the electric field. Further, the thermal history can also influence the fatigue. If a crystal can undergo a field that induces a domain state that fatigues, this ultimately controls the fatigue process, acting as a nucleation site for pinned domains in the whole crystal.

#### IV. CONCLUSIONS

All of the above illustrate the role of fatigue anisotropy and domain engineering in  $\text{Pb}(\text{Zn}_{1/3}\text{Nb}_{2/3})\text{O}_3\text{-PbTiO}_3$  crystals. Fatigue is induced if a polarization vector is normal to the electrode plane and is parallel to the electric field vector. Fatigue rates are suppressed in some directions, provided the thermal energy can overcome pinning effects or alter active nucleation probability at the electrode interface without inducing polarization parallel to the applied field. In the compositions close to the MPB, alternating electric fields can induce a ferroelectric phase with polarization parallel to the electric field direction, e.g., a rhombohedral to tetragonal phase transition in a  $[001]_C$  crystal. This then can give rise to polarization fatigue. In special directions, such as  $[110]_C$ , a rhombohedral phase can be field induced into a metastable orthorhombic phase that has polarization parallel to the normal of the electrode plane and thereby undergo fatigue. In the case of electric fields inducing mixed ferroelectric phases, the fatigue is dominated by the polarization direction parallel to the electric field direction. It is hypothesized that if a ferroelectric crystal with a relaxor end member has engineered domains with polarization inclined to the electrode normal, charge injection is either reduced and/or charge is redistributed, and/or domain switching mobility is enhanced, thereby limiting fatigue.

A comprehensive mechanism that explains fatigue is still awaiting the ferroelectrics community, however, these studies on ferroelectric phase and orientation, builds up the experimental background that ultimately has to be explained in a complete fatigue model.

#### ACKNOWLEDGMENTS

This work was achieved with the financial support of The Ministry of Turkish National Education and DARPA single crystal fund (Grant No. N00014-98-1-0527). The authors would like to thank Professor T. R. Shrout and Dr. S.-E. Park for helpful suggestions, and H. Lei and P. Wu for supplying single crystals.

- <sup>1</sup>W. J. Merz and J. R. Anderson, *Bell Lab. Rec.* **33**, 335 (1955).
- <sup>2</sup>J. R. Anderson, G. W. Brady, W. J. Merz, and J. P. Remeika, *J. Appl. Phys.* **26**, 1387 (1955).
- <sup>3</sup>H. L. Stadler, *J. Appl. Phys.* **29**, 743 (1958).
- <sup>4</sup>D. S. Campbell, *Philos. Mag.* **79**, 1157 (1962).
- <sup>5</sup>F. Jona and G. Shirane, *Ferroelectric Crystals* (Pergamon, Oxford, 1962).
- <sup>6</sup>R. Williams, *J. Phys. Chem. Solids* **26**, 399 (1965).
- <sup>7</sup>E. Fatuzzo and W. J. Merz, *Ferroelectricity* (Wiley, New York, 1967).
- <sup>8</sup>J. F. Scott and C. A. Pas de Araujo, *Science* **246**, 140 (1989).
- <sup>9</sup>W. L. Warren, D. Dimos, B. A. Tuttle, R. D. Nasby, and G. E. Pike, *Appl. Phys. Lett.* **65**, 1018 (1994).
- <sup>10</sup>W. L. Warren, D. Dimos, B. A. Tuttle, G. E. Pike, R. W. Schwartz, P. J. Clews, and P. C. McIntyre, *J. Appl. Phys.* **77**, 6695 (1995).
- <sup>11</sup>J. F. Scott, *J. Phys. Chem. Solids* **57**, 1439 (1996).
- <sup>12</sup>W. C. Stewart and L. S. Cosentino, *Ferroelectrics* **1**, 149 (1970).
- <sup>13</sup>K. Amanuma, T. Hase, and Y. Miyasaka, *Jpn. J. Appl. Phys., Part 1* **33**, 5211 (1994).
- <sup>14</sup>I. K. Yoo, S. B. Desu, and J. Xing, in *Ferroelectric Thin Films III*, MRS Symp. Proc. Vol. 310, edited by B. A. Tuttle, E. R. Myers, S. B. Desu, and P. K. Larsen (Materials Research Society, Pittsburgh, PA, 1993), p. 165.
- <sup>15</sup>D. P. Vijay and S. B. Desu, *J. Electrochem. Soc.* **140**, 2640 (1993).
- <sup>16</sup>T. Nakamura, Y. Nakano, A. Kanisawa, and H. Takasu, *Jpn. J. Appl. Phys., Part 1* **33**, 5207 (1994).
- <sup>17</sup>H. N. Al-Shareef, K. R. Bellu, A. I. Kingon, and O. Auciello, *Appl. Phys. Lett.* **66**, 239 (1995).
- <sup>18</sup>T. Nakamura, Y. Nakao, A. Kanisawa, and H. Takasu, *Appl. Phys. Lett.* **65**, 1522 (1994).
- <sup>19</sup>K. Kushida-Abdelghafar, M. Hiratani, and Y. Fujisaki, *J. Appl. Phys.* **85**, 1069 (1999).
- <sup>20</sup>J. T. Cheung, P. E. D. Morgan, and R. Neurgaonkar, *Proceedings of the 4th International Symposium on Integrated Ferroelectrics*, Colorado Springs, CO, 1992, p. 518.
- <sup>21</sup>R. Ramesh, H. Girchlist, T. Sands, V. G. Keramidis, R. Haakenaasen, and D. K. Fork, *Appl. Phys. Lett.* **63**, 3592 (1993).
- <sup>22</sup>C. B. Eom, R. B. V. Dover, J. M. Phillips, D. J. Werder, J. H. Marshall, C. H. Chen, R. M. Fleming, and D. K. Fork, *Appl. Phys. Lett.* **63**, 2570 (1993).
- <sup>23</sup>J. Yin, T. Zhu, Z. G. Liu, and T. Wu, *Appl. Phys. Lett.* **75**, 3698 (1999).
- <sup>24</sup>S. Aggarwal, I. G. Jenkins, B. Nagaraj, C. J. Kerr, C. Canedy, R. Ramesh, G. Valasquez, L. Boyer, and J. T. Evans, Jr., *Appl. Phys. Lett.* **75**, 1787 (1999).
- <sup>25</sup>R. Dat, J. K. Lee, O. Auciello, and A. I. Kingon, *Appl. Phys. Lett.* **67**, 572 (1995).
- <sup>26</sup>C. A. Pas de Araujo, J. D. Cuchiaro, L. D. McMillian, M. C. Scott, and J. F. Scott, *Nature (London)* **374**, 627 (1995).
- <sup>27</sup>K. Takemura, M. Ozgul, V. Bornand, S. Trolier-McKinstry, and C. A. Randall, *Proceedings of the 9th US-Japan Workshop on Dielectric and Piezoelectric Ceramics*, Okinawa, Japan, 1999.
- <sup>28</sup>V. Bornand, S. Trolier McKinstry, K. Takemura, and C. A. Randall, *J. Appl. Phys.* **87**, 3965 (2000).
- <sup>29</sup>K. Takemura, M. Ozgul, V. Bornand, S. Trolier-McKinstry, and C. A. Randall, *J. Appl. Phys.* **88**, 7272 (2000).
- <sup>30</sup>C. A. Randall, A. S. Bhalla, T. R. Shrout, and L. E. Cross, *J. Mater. Res.* **5**, 829 (1990).
- <sup>31</sup>S.-E. Park and T. R. Shrout, *Mater. Res. Innovations* **1**, 20 (1997).
- <sup>32</sup>M. L. Mulvihill, S.-E. Park, G. Rish, and T. R. Shrout, *Jpn. J. Appl. Phys., Part 1* **35**, 561 (1996).
- <sup>33</sup>J. Kuwata, K. Uchino, and S. Nomura, *Ferroelectrics* **37**, 579 (1981).
- <sup>34</sup>S.-F. Liu, S.-E. Park, T. R. Shrout, and L. E. Cross, *J. Appl. Phys.* **85**, 2810 (1999).
- <sup>35</sup>H. Yu and C. A. Randall, *J. Appl. Phys.* **86**, 5733 (1999).
- <sup>36</sup>H. Yu, V. Gopalan, J. Sindel, and C. A. Randall, *J. Appl. Phys.* **89**, 561 (2001).